

# Modified Structure of Photonic Crystal Fiber with Dispersion and Confinement Loss Properties for Wideband Applications

<sup>1</sup>Kubra Bashir, <sup>2</sup>Rabia Zaman, <sup>3</sup>Seema Ansari

<sup>1,2,3</sup> Department of Electrical Engineering, Institute of Business Management, Karachi Pakistan

<sup>1</sup>[kubra.bashir@iobm.edu.pk](mailto:kubra.bashir@iobm.edu.pk)

<sup>2</sup>[rabia.zaman@iobm.edu.pk](mailto:rabia.zaman@iobm.edu.pk)

<sup>3</sup>[seema.ansari@iobm.edu.pk](mailto:seema.ansari@iobm.edu.pk)

**Abstract:** In this article, an optimized structure of Photonic Crystal Fiber (PCF) has been planned that investigates the effect of dispersion and confinement loss of square shaped photonic crystal fiber, intended for wideband applications ranges from 1.35um to 1.70um. The objective of the suggested geometry is to attain such optical properties by fluctuating its parameters like pitch, number of outer circular rings and inner elliptical rings to make it flexible and simple for manufacturing. Finite Element Method and Perfectly Matched Boundary layer (PML) is set for this proposed geometry. Moreover, recommended PCF structure has unlimited application value in the fiber-optic communications such as fiber lasers, highly sensitive gas sensors, nonlinear devices, high-power transmission and much more.

**Keywords**—Confinement Loss (CL); Finite Element Method (FEM); Perfectly Matched Boundary layer (PML).

## I. INTRODUCTION

The knowledge of a photonic crystal fiber was first offered by Yeh et al. [1] in 1978.

Photonic Crystal fibers are observed a favorable fiber technology that yields some exceptional features like controllable non-linearity, dispersion [2,3,4] and endless single mode [2]. PCF structure can be designed more flexible way with desired optical characteristics when compared with conventional fibers [5,6]. As discussed in [7], a PCF requires transmission ability that confirms a low confinement loss (CL), low cross talk, large mode area and low dispersion.

According to one of the researches by to Broeng J and Knight J C, the impact of modeling parameters on optical characteristics of PCF has been discussed in [8,9]. Several other researches about Dispersion Compensating Fiber DCF which exhibits large negative dispersion. [10-15]. A. A Nair and S.K.Singh examined several impressive properties like dispersion, confinement loss, effective area, non-linearity etc. through suitable selection of holes diameter, pitch constant ( $\Lambda$ ), number of rings ( $N_r$ ), and arrangement of air holes

mentioned in [16-17]. Another reported research on low dispersion and low confinement loss by changing PCF structure is observed by H. Ademgil and S. Haxha, in [18].

Dispersion is one of the pitfalls in PCF. To overcome this hazard many techniques have been used earlier to get flattened dispersion like by varying air holes shape, air holes diameter and filling of air holes with different liquids and gases as revealed in [19-22]. In previous researches, a hexagonal geometry using Silica with five number of rings by has been observed in [23] and A square lattice PCF structure is inspected in [24-25]. Furthermore, a single mode PCF using octagonal lattice is discussed in [26].

and other geometries with higher nonlinearity are mentioned in [27-31]. PCF adjustments in structural parameters with zero dispersion and dispersion shifted fibers are discussed in [32].

In previous work of 2019, we have analyzed a square lattice PCF structure by means of Silica and Borosilicate crown glass as their core materials and extracted optical properties like confinement loss and dispersion, also discussed the effect of diameter of air holes [33].

This research is the expansion based on the prior literature [13]. Now we further investigated the potential in same Square lattice geometry using only Silica as a core material, consists of inner elliptical and outer circular air hole rings and studied the impact of parameters like Number of rings  $N_r$ , Major axis ( $a$ ) and Minor axis ( $b$ ) of elliptical air holes focused on same geometry discussed [34].

## II. NUMERICAL ANALYSIS

### 1. Chromatic Dispersion:

The chromatic dispersion  $D$  can be determined from the  $n_{eff}$  values versus the wavelength from the given formula mentioned in [35].

$$D = -\frac{\lambda}{c} \frac{d^2 Re[n_{eff}]}{d\lambda^2} \quad (1)$$

where  $c$  is the velocity of light in a vacuum,  $\lambda$  is wavelength of the light in fiber. and  $Re$  stands for the real part and  $(n_{eff})$  is the effective refractive index of the mode can be obtained by calculating the Eigen value of Maxwell's equation in [23] and [34]. The material dispersion is calculated by given Sellmeier's formula in [36].

$$n(\lambda) = S_0 - S_1\lambda^2 - S_2\lambda^4 + \frac{S_3}{C} - \frac{S_4}{C^2} + \frac{S_5}{C^3} \quad (4)$$

Where  $S_{1,2,3,4,5}$  are the experimentally determined Sellmeier's coefficients given as.

$$S_0 = 1.4508554, S_1 = 0.0031268, S_2 = 0.0000381,$$

$$S_3 = 0.0030270, S_4 = 0.0000779, S_5 = 0.0000018$$

$$C = \lambda^2 - 0.035$$

### 2. Confinement Loss:

The loss produced by the waveguide geometry is a confinement loss  $L_c$ . Its an additional loss arises in single-material fibers mainly in PCFs because they are usually made of pure silica given in [37].

$$CL = 8.686 \frac{2\pi}{\lambda} \text{Im}[n_{eff}] \quad \left[ \frac{dB}{m} \right] \quad (3)$$

## III. PCF DESIGN

The proposed PCF structure consists of total five number of air holes rings (Nr) including the elliptical inner holes with major axis ( $a$ ), and minor axis ( $b$ ) and outer circular rings with diameter ( $d$ ) solid core and hole-hole spacing (pitch).

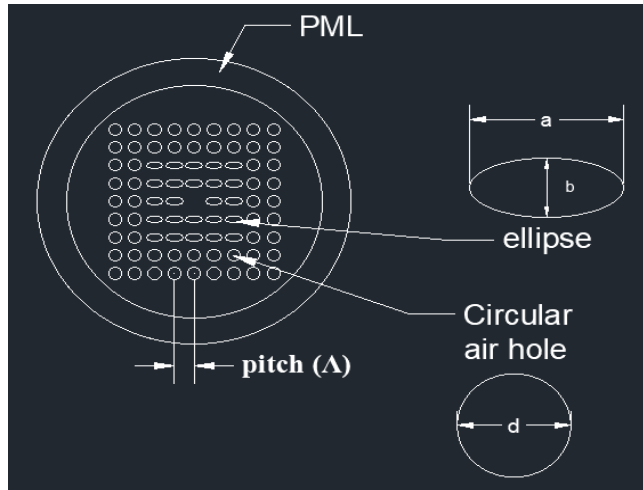


**Fig. (1).** Geometry of proposed square lattice PCF of with inner elliptical rings with major axis  $a$  ( $\mu\text{m}$ ) and minor axis  $b$  ( $\mu\text{m}$ ) and outer circular rings with diameter  $d$  in  $\mu\text{m}$  and pitch  $\Lambda$  in  $\mu\text{m}$ .

This design is modelled using the following steps given below.

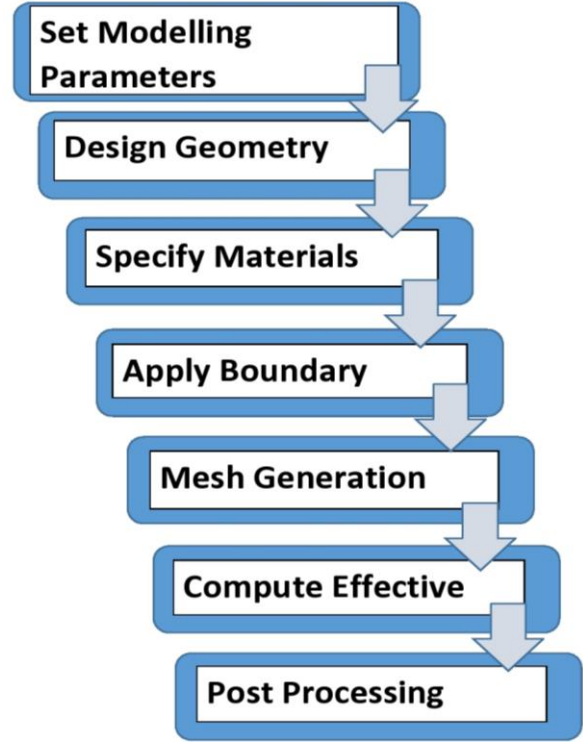


**Fig. (2).** Simulation steps of modelling PCF Structure.

## IV. RESULTS & DISCUSSIONS

The effect of both dispersion and confinement loss is investigated in various cases by selected the main features mentioned below, carried out in the wavelength ranges from 1.1 to 1.8  $\mu\text{m}$ .

*Case I-* In this case, minor axis is carefully chosen particularly at  $b=0.1\mu\text{m}$ ,  $0.2\mu\text{m}$  and  $0.3\mu\text{m}$  and the initially considered values are:  $d=1.0\mu\text{m}$  diameter of the circular air hole, pitch is  $\Lambda=2.3\mu\text{m}$  and major axis  $a=0.4\mu\text{m}$ .

Figure 3 demonstrate the dispersion effect for the above discussed case. It can be clearly observed that due to the increase in minor axis  $b$  the dispersion effect is nearly zero.

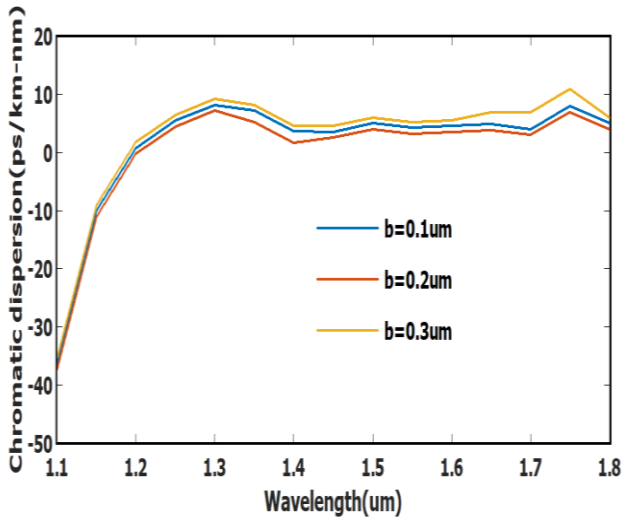


Fig. (3). Plot of chromatic dispersion variation due to change of minor axis  $b$  at  $d=1.0\mu\text{m}$ ,  $\Lambda=2.3\mu\text{m}$ ,  $a=0.4\mu\text{m}$ .

Figure 4 shows the effect of confinement loss for the same case. It is obvious from this profile that the confinement loss is continuously moving upward with the increase in minor axis.

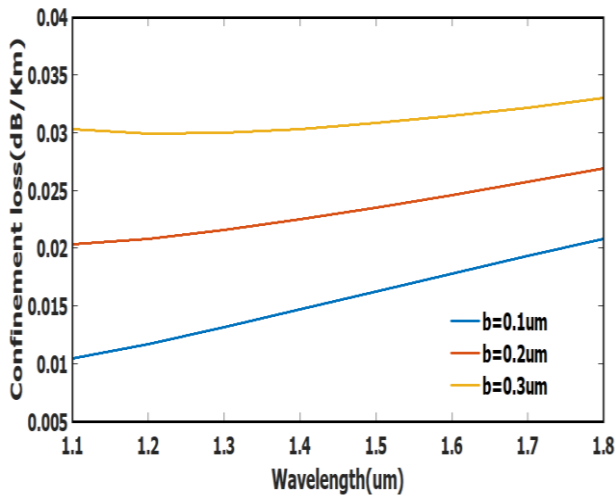


Fig. (4). Plot of confinement loss variation due to change of minor axis  $b$  at  $d=1.0\mu\text{m}$ ,  $\Lambda=2.3\mu\text{m}$ ,  $a=0.4\mu\text{m}$ .

*Case II-* In this case, major axis is selected particularly at  $a=0.3\mu\text{m}$ ,  $0.4\mu\text{m}$  and  $0.5\mu\text{m}$  and the primarily considered values are:  $d=1.0\mu\text{m}$  diameter of the circular air hole, pitch is  $\Lambda=2.3\mu\text{m}$  and minor axis  $a=0.1\mu\text{m}$ .

In Figure 5 dispersion effect can be analyzed for the above discussed case. We observed that due to the slight increase in major axis, numerous effects can be investigated. It can be noticed that the solid red line represents the flat dispersion in the range from  $1.4\mu\text{m}$  to  $1.7\mu\text{m}$  and before that it has negative dispersion which is being used a Dispersion Compensating Fiber. [13] whereas at major axis  $0.5\mu\text{m}$  it goes all the way down towards negative dispersion.

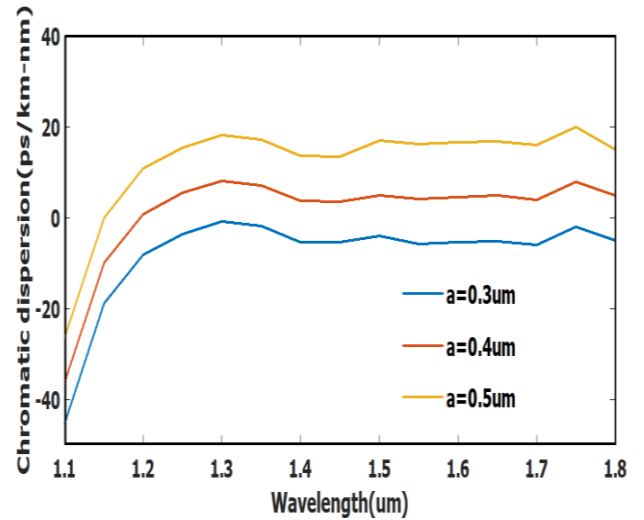


Fig. (5). Plot of chromatic dispersion variation due to change of major axis  $a$  at  $d=1.0\mu\text{m}$ ,  $\Lambda=2.3\mu\text{m}$ ,  $b=0.1\mu\text{m}$ .

Figure 6 gives the information about confinement loss for the same case. This line graph is clearly identifying that the confinement loss varies due to the variation in major axis.

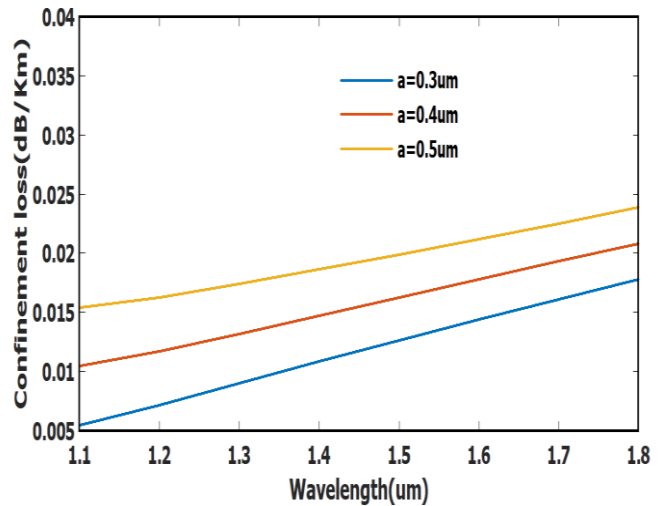


Fig. (6). Plot of confinement loss variation due to change of major axis  $a$  at  $d=1.0\mu\text{m}$ ,  $\Lambda=2.3\mu\text{m}$ ,  $b=0.1\mu\text{m}$ .

*Case III-* In this case  $d=1.0\mu\text{m}$  diameter of the circular hole, major axis  $a=0.4\mu\text{m}$ , minor axis  $b=0.1\mu\text{m}$  are kept constant and pitch between air holes are efficiently selected at  $2.1\mu\text{m}$ ,  $2.3\mu\text{m}$  and  $2.5\mu\text{m}$ .

Figure 7 displays the dispersion profile as it is attracting more towards zero dispersion that is consistent between  $1.4\mu\text{m}$  to  $1.7\mu\text{m}$  wavelengths at pitch value  $2.1\mu\text{m}$  and  $2.3\mu\text{m}$  but as the value of pitch varies to  $2.5\mu\text{m}$ , the dispersion will excite rapidly.

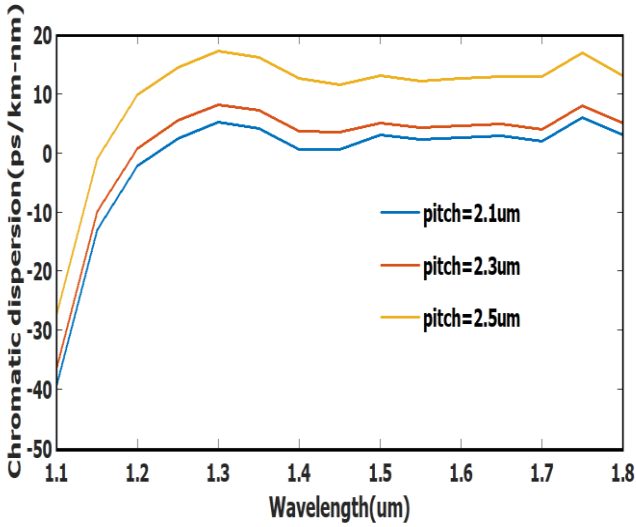


Fig. (7). Plot of chromatic dispersion variation due to change of pitch ( $\Lambda$ ) at  $d=1.0\mu\text{m}$ ,  $a=0.4\mu\text{m}$ ,  $b=0.1\mu\text{m}$ .

Figure 8 is a clear demonstration of confinement loss as it providing the lowest loss with respect to the increase in pitch. Due to this attractive feature it becomes more striking as comparable to the losses we calculated earlier.

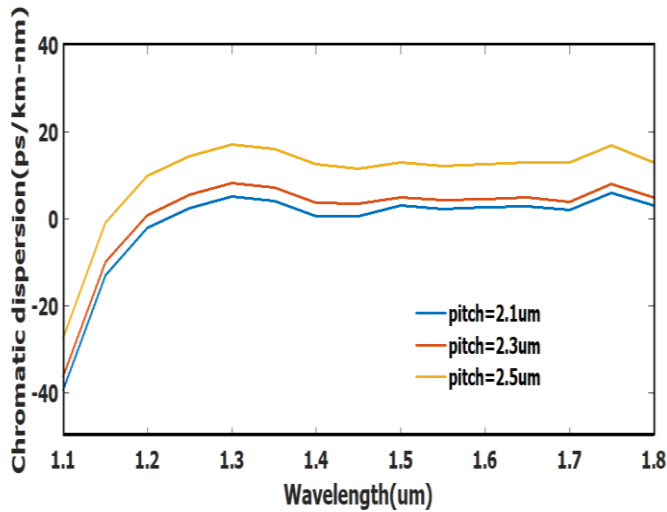


Fig. (8). Plot of confinement loss due to change of pitch ( $\Lambda$ ) at  $d=1.0\mu\text{m}$ ,  $a=0.4\mu\text{m}$ ,  $b=0.1\mu\text{m}$ .

*Case IV-* This case shows the working on number of circular rings  $N_r$  randomly selected at 4, 5 and 6 whereas rest of parameters priory discussed i-e diameter of the circular hole  $d=1.0\mu\text{m}$ , major axis  $a=0.4\mu\text{m}$ , minor axis  $b=0.1\mu\text{m}$  and pitch= $2.3\mu\text{m}$  are kept constant.

The plot shown below in figure 9 demonstrates the dispersion effect achieved due to the increased number of circular rings. This case gives the information that when the number of rings is selected 4, dispersion is high, at  $N_r=5$  dispersion tends to nearly zero (flat dispersion) and at  $N_r=6$  it reaches towards negative dispersion.

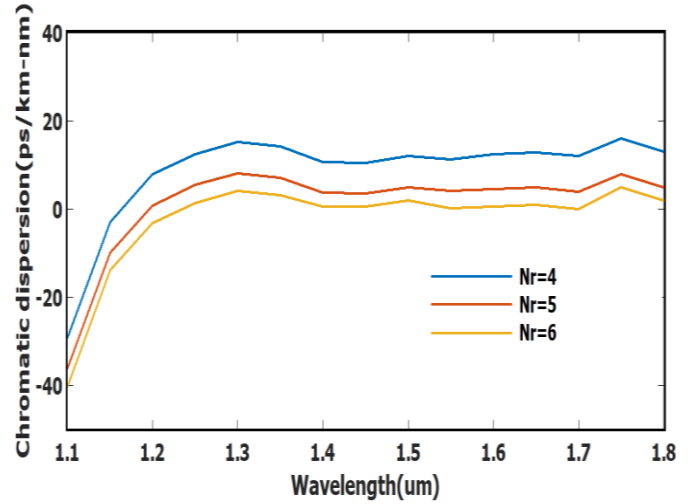


Fig. (9). Plot of chromatic dispersion variation due to change of number of circular rings  $N_r$  at  $d=1.0\mu\text{m}$ ,  $\Lambda=2.3\mu\text{m}$ ,  $a=0.4\mu\text{m}$ ,  $b=0.1\mu\text{m}$ .

Confinement loss also falling-off as we are increasing the number of circular rings shown in Figure 10.

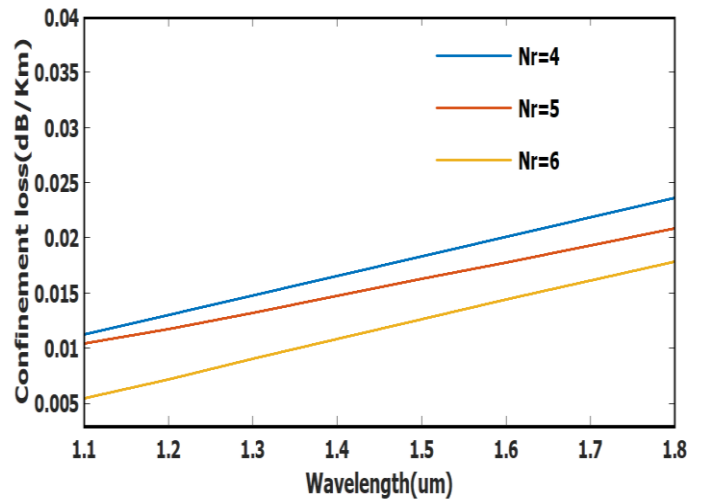


Fig. (10). Plot of confinement loss variation due to change of number of circular rings  $N_r$  at  $d=1.0\mu\text{m}$ ,  $\Lambda=2.3\mu\text{m}$ ,  $a=0.4\mu\text{m}$ ,  $b=0.1\mu\text{m}$ .

*Case V-* This case gives the information about chromatic dispersion and confinement loss, arises due to the variation in number of elliptical air rings  $N_r$  chosen at 4, 5 and 6 whereas all other parameters diameter of the circular hole  $d=1.0\mu\text{m}$ , major axis  $a=0.4\mu\text{m}$ , minor axis  $b=0.1\mu\text{m}$  and pitch= $2.3\mu\text{m}$  are kept constant.

In Figure 11 it can be easily observed that increased number of elliptical rings providing us the positive response that are heading towards flat dispersion with respect to the smaller number of rings.

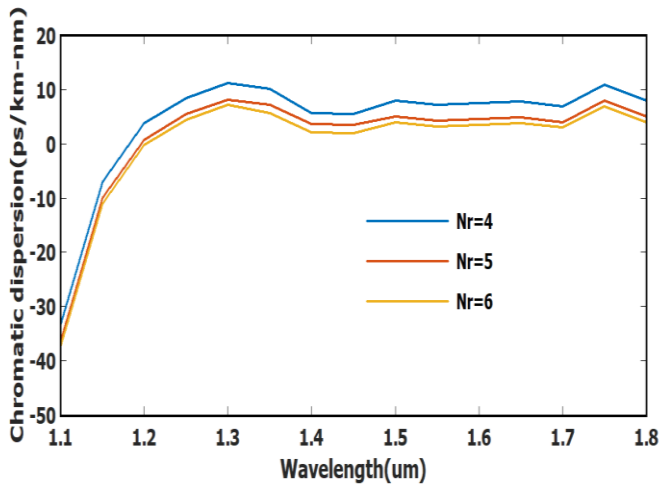


Fig. (11). Plot of chromatic dispersion variation due to change of number of elliptical rings  $N_r$  at  $d=1.0\mu\text{m}$ ,  $\Lambda=2.3\mu\text{m}$   $a=0.4\mu\text{m}$ ,  $b=0.1\mu\text{m}$ .

In Figure 12 it can be noted that Confinement loss is inversely proportional to the number of elliptical rings. The loss is dropped rapidly as we increased the number of elliptical rings.

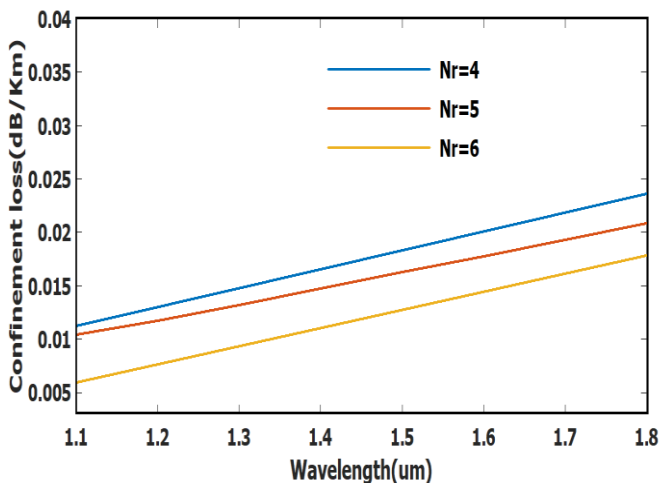


Fig. (12). Plot of confinement loss variation due to change of number of elliptical rings  $N_r$  at  $d=1.0\mu\text{m}$ ,  $\Lambda=2.3\mu\text{m}$   $a=0.4\mu\text{m}$ ,  $b=0.1\mu\text{m}$ .

## V. CONCLUSION

This article is the modified version of our previous work, in which effect of both chromatic dispersion and confinement loss has been investigated on square lattice PCF with wavelength ranges 1.1-1.8 $\mu\text{m}$ , under the influence of different parameters like pitch between two holes, number of circular and elliptical rings, variation in sizes of circular and elliptical holes. These results demonstrate that the optimized PCF performs very well and accomplishes great progress in terms of dispersion and confinement loss. Finally, we can say that these

parameters can be adjustable based on the applications requirement. Besides, the proposed structure can be operated over the vastly usable communication applications such as fiber lasers, nonlinear devices, high-power transmission, highly sensitive gas sensors, and other areas.

## REFERENCES

- [1] Pochi Yeh, Amnon Yariv, and Emanuel Marom, "Theory of Bragg fibers," *J. Opt. Soc. Am.* 68, 1196-1201 (1978). <https://doi.org/10.1364/JOSA.68.001196>
- [2] Uebel P, Gu "nendi Mehmet C, Frosz MH, "Broadband robustly single-mode hollow-core PCF by resonant filtering of higher-order modes". *Opt. Lett.* 2016 May; 41(9):1961–1964. <https://doi.org/10.1364/OL.41.001961> PMID: 27128049.
- [3] Amezcua-Correa R, Broderick NGR, Petrovich MN, et al, "Design of 7 and 19 cells core air-guiding photonic crystal fibers for low-loss, wide bandwidth and dispersion-controlled operation," *Opt. Express.* 2007 Dec; 15(26):17577–17586. <https://doi.org/10.1364/oe.15.017577> PMID: 19551052.
- [4] Islam M I, Khatun M, Ahmed K, Asaduzzaman S, Paul B K, Islam M S, Chowdhury S, Sen S, Miah M B A, Bahar A N, "Design and analysis of single-mode PCF in optical communication covering E to L bands with ultra-high negative dispersion," *Ukrainian Journal of Physics*, 2017, 62(9): 818–826.
- [5] R. Buczynski, "Photonic Crystal Fibers", vol.106, International School of Semiconducting Compounds, Jaszowiec 2004.
- [6] Partha Sona Maji, Partha Roy Chaudhuri, "A new design of ultra-flattened near-zero dispersion PCF using selectivity liquid infiltration," arXiv:1412.7846, 2014.
- [7] Geng Z, Wang N, Li K, Kang H, Xu X, Liu X, et al. (2020), "A Photonic crystal fiber with large effective refractive index separation and low dispersion," *PLoS ONE* 15(5): e0232982. <https://doi.org/10.1371/journal.pone.0232982>
- [8] Broeng J, Mogilevstev D, Barkou S E, Bjarklev, "Photonic crystal fibers: a new class of optical waveguides," *Optical Fiber Technology*, 1999, 5(3): 305–330 <https://doi.org/10.1006/ofte.1998.0279>.
- [9] Knight J C. Photonic crystal fibres. *Nature*, 2003, 424: 847–851 <https://doi.org/10.1038/nature01940>
- [10] Gr"uner-nielsen L, Wandel M, Kristensen P, J"orgensen C, J"orgensen L V, Edvold B, P"alsd"ottir B, Jakobsen D, "Dispersion-compensating fibers," *Journal of Lightwave Technology*, Vol. 23, 2005.
- [11] K. Saitoh, M. Koshiba, T. Hasegawa, and E. Sasaoka, "Chromatic dispersion control in photonic crystal fibers: application to ultra-flattened dispersion," *Opt. Express* 11, 843–852 (2003).

- [12] Kaijage S F, Namihira Y, Hai N H, Begum F, Razzak S M A, Kinjo T, Miyagi K, Zou N, "Broadband dispersion compensating octagonal photonic crystal fiber for optical communication applications," *Japanese Journal of Applied Physics*, 2009, 48(5): 052401  
<https://doi.org/10.1143/JJAP.48.052401>
- [13] Kubra Bashir and Rabia Zaman, "Designing dispersion flattened photonic crystal fiber for wideband applications," *Journal of independent studies and research-computing*, Vol 17 No 1 (2019). January-June.
- [14] Islam M I, Khatun M, Ahmed K, "Ultra-high negative dispersion compensating square lattice based single mode photonic crystal fiber with high nonlinearity," *Optical Review*, 2017, 24(2): 147–155  
DOI 10.1007/s10043-017-0308-0
- [15] Islam, M.I., Ahmed, K., Paul, B.K. *et al.* Ultra-high negative dispersion and nonlinearity based single mode photonic crystal fiber: design and analysis. *J Opt* 48, 18–25 (2019).  
<https://doi.org/10.1007/s12596-018-0499-1>
- [16] A.A Nair, S. Sudheer and M. Jayaraju, "Analysis of Optical Characteristics for Photonic Crystal fiber at small core Diameters," *International Journal of Engineering and Advanced Technology (IJEAT)*, vol. 3, Issue-4, 2014.  
DOI=10.1.1.675.6324
- [17] S.K. Singh, D. Singh and P. Mahto, "Tailoring of Flattened Dispersion in Triangular-Lattice Photonic Crystal Fiber," *International Journal of Distributed and Parallel Systems*, vol. 2, p:127, 2011.  
DOI: 10.5121/ijdps.2011.2612
- [18] H. Ademgil and S. Haxha, "Highly Birefringent Photonic Crystal Fiber with Ultralow Chromatic Dispersion and Low Confinement Losses," *J. Lightwave Technol.* 26 (2008), 441–448.
- [19] Stepniewski, G., Klimczak, M., Bookey, H., Siwicki, B., Pysz, D., Stepien, R., Buczynski, R. (2014), "Broadband supercontinuum generation in normal dispersion all-solid photonic crystal fiber pumped near 1300 nm," *Laser Physics Letters*, 11(5), 055103.  
DOI:10.1088/1612-2011/11/5/055103
- [20] L.Cherbi, "Modeling of two rings photonic Crystal Fiber with scalar element method," *J. Optoelectron. Adv. Mater.* 15 (2013), no.11-12, 1385-1391.
- [21] Poletti, F., Finazzi, V., Monro, T. M., Broderick, N. G. R., Tse, V., & Richardson, D. J. (2005), "Inverse design and fabrication tolerances of ultra-flattened dispersion holey fibers," *Optics Express*, vol.13, no.10, 3728.  
DOI:10.1364/ope.13.003728
- [22] Ferhat, M. L., Cherbi, L., & Haddouche, I. (2018), "Supercontinuum generation in silica photonic crystal fiber at 1.3  $\mu\text{m}$  and 1.65  $\mu\text{m}$  wavelengths for optical coherence tomography," *Optik*, 152, 106–115.  
DOI: 10.1016/j.ijleo.2017.09.111
- [23] Jay Prakash Vijay and Md. Sabir, "Low Flattened Dispersion Hexagonal Photonic Crystal Fiber with Low Confinement Loss," *International Journal of Emerging Technology and Advanced Engineering*, 2008 Certified Journal, vol. 3, Issue 1, Jan 2013.
- [24] Archana Mahur and Yogendra Kumar Katiyar, "Flattened Dispersion in Square Lattice Photonic Crystal Fiber of Borosilicate Material with Square & Circular Air Holes," *International Journal of Advanced Engineering Research & Science (IJAERS)*, vol.1, Issue-1, June 2014.
- [25] Z.L Liu et al., "Characteristics of a large negative dispersion and low confinement losses PCF," *Semicond. Optoelectron* 2008.
- [26] Florous, N., Saitoh, K., & Koshiba, M. (2006), "The role of artificial defects for engineering large effective mode area, flat chromatic dispersion, and low leakage losses in photonic crystal fibers: Towards high speed reconfigurable transmission platforms," *Optics Express*, 14(2), 901.  
<https://doi.org/10.1364/OPEX.14.000901>
- [27] Paul, B. K., Golam Moctader, M., Ahmed, K., & Abdul Khalek, M. (2018), "Nanoscale GaP strips based photonic crystal fiber with high nonlinearity and high numerical aperture for laser applications," *Results in Physics*, 10, 374–378.  
DOI: 10.1016/j.rinp.2018.06.033
- [28] Monfared, Y. E., Liang, C., Khosravi, R., Kacerovska, B., & Yang, S. (2019), "Selectively toluene-filled photonic crystal fiber Sagnac interferometer with high sensitivity for temperature sensing applications," *Results in Physics*, 13, 102297.  
DOI: 10.1016/j.rinp.2019.102297
- [29] Monfared, Y. E., & Ponomarenko, S. A. (2019), "Extremely nonlinear carbon-disulfide-filled photonic crystal fiber with controllable dispersion," *Optical Materials*, 88, 406–411.  
DOI: 10.1016/j.optmat.2018.12.010
- [30] Monfared, Y. E., & Ponomarenko, S. A. (2016), "Slow light generation via stimulated Brillouin scattering in liquid-filled photonic crystal fibers," *Optik - International Journal for Light and Electron Optics*, 127(15), 5800–5805.  
DOI: 10.1016/j.ijleo.2016.04.017
- [31] Saitoh, K., Koshiba, M., Hasegawa, T., & Sasaoka, E. (2003), "Chromatic dispersion control in photonic crystal fibers: Application to ultra-flattened dispersion," *Optics Express*, 11(8), 843.  
DOI:10.1364/oe.11.000843
- [32] Tzong-Lin Wu, & Chia-Hsin Chao. (2005), "A novel ultra-flattened dispersion photonic Crystal fiber," *IEEE Photonics Technology Letters*, 17(1), 67–69.  
DOI:10.1109/lpt.2004.837475
- [33] Shish Ram, Ritu Sharma and Vijay Jangyani, "Comparison of Dispersion properties for different lattice of Photonic Crystal Fiber," *International journal of Computer Applications on Electronics, Information and Communication Engineering ICEICE* no.3, Dec 2011.
- [34] Faruk, M.M., Khan, N.T. & Biswas, S.K. Highly nonlinear bored core hexagonal photonic crystal fiber (BC-HPCF) with ultra-high negative dispersion for fiber optic transmission system. *Front. Optoelectronics*. (2019).  
<https://doi.org/10.1007/s12200-019-0948-8>
- [35] Shish Ram, Ritu Sharma, Vijay Janyani and Rotash Kumar. Article: Comparison of Dispersion Properties for Different Lattice of Photonic Crystal Fiber. *IJCA Special Issue on Electronics, Information and Communication Engineering ICEICE* (3):4-7, December 2011.
- [36] Gautam Prabhakar, Akshit Peer, Ajeet Kumar and Vipul Rastogi, "Finite element analysis of solid-core Photonic crystal fiber," *IEEE* 2012.  
DOI: 10.1109/SCES.2012.6199068

- [37] Hossain, Md & Maniruzzaman, Md. (2015). Study of Confinement Loss in Photonic Crystal Fiber. International Conference on Materials, Electronics & Information Engineering, ICMEIE-2015 05-06 June, 2015, Faculty of Engineering, University of Rajshahi, Bangladesh

[32]